Nigerian Journal of Mathematics and Applications
Volume **32** (**II**), (2022), 293 – 314. *Printed by Unilorin press*
©*Nig. J. Math. Appl.* *http : //www.njmaman.com*

Special Issue in Honor of Prof. J. A. Gbadeyan's Retirement

MHD Free Convection Flow of Viscoelastic Fluid Through a Vertical Porous Plate with Thermal Conductivity under Soret-Dufour Influence

A. S. Idowu[1*], Abdulwaheed Jimoh[2] and Ahmed Lukman[3]

Abstract

A study of MHD heat and mass transfer of viscoelastic fluid past a porous plate with thermal conductivity under soret-dufour effect is investigated. The governing boundary-layer equations are formulated with appropriate boundary conditions. The Roseland diffusion approximation is used to analyze the radiative heat flux and it is appropriate for non-Scattering media. The governing boundary layer equations were simplified and non-dimensional equation. The dimensionless equations were discretized and then solved using the Crank-Nicolson's method. The velocity, temperature and concentration distributions are derived and discussed numerically and in tabular forms. It is observed that velocity increases with the increase in Gr (Grashof number), Jeffery fluid parameter and magnetic field M parameter but it decreases with the increase in Fs and Da.

1. Introduction

The study of heat and mass transfer magneto hydrodynamic of viscoelastic fluid past a vertical porous plate with thermal conductivity and chemical reactions effects has attracted the interest of a considerable number of researchers because of its numerous applications in several branches of science and engineering and in transport processes. Heat and mass transfer problem in a porous medium has important applications in geothermal reservoir, geothermal extraction and heat exchangers. These applications in industries include drying, cooling of nuclear reactors chemical deposition on surfaces and magneto hydrodynamic (MHD) power generators, solar physics, astrophysical studies and polymer technology.

Received: 21/10/2022, Accepted: 10/11/2022, Revised: 02/12/2022. * Corresponding author.
2015 *Mathematics Subject Classification.* 37C10 & 80A19.
Keywords and phrases. Free Convection, MHD flow, Porous medium, Vertical plate, Kuvshinshiki fluid and Soret-Dufour
[1]Department of Mathematics, University of Ilorin, Ilorin, Nigeria
[2]Nigerian Communication Satellite Limited, Airport Road, Lugbe, Abuja, Nigeria
[3]Department of Mathematical Sciences, Baze University, Abuja, Nigeria
E-mails of the corresponding author: sesan@unilorin.edu.ng
ORCID of the corresponding author: 0000-0002-5634-3449

Fluids in which shear stress is not proportional to the deformation are known as non-Newtonian fluids. Non-Newtonian fluids are classified into two main classes; differential type fluids and rate type fluids. In the category of non-Newtonian fluids, viscoelastic of Kuvshinshiki fluid is one of the very few studies which have not been investigated on heat and mass transfer characteristics in the presence of applied uniform magnetic field. Also this type of flow is very common in petroleum engineering which are concerned with movement of oil, gas and water through reservoir of oil or gas field and in hydrologist involving the study of the migration of underground water. In chemical engineering for the purification and filtration processes and industry for determination of drug permeation through human skin. The principle of this subject is very useful in recovering water for drinking and irrigation purposes. Finite difference method was applied in the study of an unsteady mixed convection flow past a semi-infinite vertical permeable moving plate with heat and mass transfer in the presence of radiation and viscous dissipation by Latha et al (2012), the presence of Eckert number effects leads to an increase skin-friction and decrease in Nusselt number. Also, Rushi et al. (2012) have considered the impact of MHD viscoelastic non-Darcy fluid flow along vertical cone using perturbation analysis, the results indicate that the Soret and Dufour effects have considerable effect on the viscoelastic fluid flow through non-Darcy porous medium. Sarada et al. (2013) examined the effects of Soret and Dufour on an unsteady MHD free convention flow past a vertical porous plate in the presence of suction or injection with aid of numerical method of Crank-Nicolson method, the result shows that as dufour number (Du) increases there is an increase in temperature distribution.

Mohan et al. (2013), considered the effect of chemical reaction and radiation on MHD free convection flow of Kuvshinshiki fluid through a vertical porous plate with heat sources by using perturbation method, It is observed that velocity, temperature profiles are more influenced by effects physical parameters.

In another study, Idowu and Jimoh et al. (2017), examined the effect of thermal conductivity on magneto-hydrodynamic heat and mass transfer in porous medium saturated with Kuvshinshiki fluid using numerical approach. The numerical results revealed that the visco-elastic Kuvshinshiki fluid type is growing as concentration profile increases, while the velocity and temperature profile falls, as the radiation and thermal conductivity were growing as velocity and temperature increases. Gnaneswara et al. (2011) numerically examine the finite element analysis of Soret and Dufour effects on unsteady Mhd free convection flow past an impulsively started vertical porous plate with viscous dissipation. The result revealed that an increase in the Dufour number causes a rise in the velocity and temperature throughout the boundary layer.

Free convective flow is a significant factor in several practical applications, cooling of electronic components, in design related to thermal insulation, material processing and geothermal systems, among others. Transient natural convection is of fundamental interest in many sciences and engineering. This frequently occurs in petro-chemical industry, power and cooling systems, air conditioning systems, atmospheric flows, motors, thermal regulation process, and security of energy systems, etc. Vidyasagar et al. (2013) considered an unsteady MHD free convection boundary layer flow of radiation absorbing Kuvshinshiki fluid through porous medium. It was shown that the concentration profile was observed to decreased when chemical reaction parameter Kr and Schmidt number Sc increases. Vidyasagar et al.(2015) again addressed unsteady MHD free convection flow of a viscous dissipative Kuvshinski fluid past an infinite vertical porous plate in the presence of radiation, thermal diffusion and chemical effects. The effect of magnetic field and radiation parameters was shown to accelerate

the velocity profiles using analytical approached.
Oyelami et al. (2016) in their work observed the effects of finite difference method applied to an unsteady magnetohydrodynamic Newtonian fluid with wall slip in Darcy-Forchiemer porous medium. The results revealed that the wall can be strengthened by increasing the wall slip. Perturbation technique on MHD free convection flow of Kuvshinshiki fluid with heat and mass transfer past a vertical porous plate was studied by Gupta et al (2011). Using analytical technique, it was noticed that velocity increases with increase in porosity parameter K and decreases with the increase in magnetic and Visco-elastic parameters M and λ respectively.
Heat and mass transfer problem in a porous medium has important applications in geothermal reservoirs and geothermal extractions. The phenomenon of Heat and mass transfer arises in the fluid when temperature changes cause density variation leading to buoyancy forces acting on the fluid elements. This can be seen in our everyday life in the atmospheric flow, which is driven by temperature differences. Agrawal et al. (2012) have discussed the effect of stratified viscous Kuvshinski fluid on MHD free convective flow with heat and mass transfer past a vertical porous plate. Sharma and Varshney (2013) have extended the problem of Agrawal et al. (2012) and investigated the effect of stratified Kuvshinshiki fluid on MHD free convective flow past a vertical porous plate with heat and mass transfer neglecting induced magnetic field in comparison to applied magnetic field.
A thorough examination of all the existing studies shows that combined impact of thermal conductivity, radiation, viscous dissipation, variable suction and chemical reaction on stratified magneto-hydrodynamics of viscoelastic (kuvshinshiki type) fluid flow past a vertical porous medium with heat source, thermal conductivity and chemical reaction have not received attention of researchers to the best knowledge of the author. Considering various occurrence, combined influence of viscous dissipation, thermal radiation, chemical reaction and thermal conductivity in stratified visco-elastic of MHD heat and mass transfer past a vertical porous medium, have serious important application in; the field of chemical processing industry, food processing, petroleum industry and other areas of viscous dissipation fluids. Hence, this study examined the impacts of thermal conductivity, viscous dissipation, heat source and chemical reaction on stratified visco-elastic MHD heat and mass transfer. The governing equations were formulated and transformed to dimensionless equations. Numerical solution to the transformed governing non-linear partial differential equations were obtained using Crank-Nicolson finite difference method. The equations expressed in their finite difference form Thomas algorithm tri-diagonal matrix system of equations which was solved with the help of MATLAB programming package.
Formulation of Problem. Utilizing thermal diffusion and concentrating impact, we explored the following assumptions: an instable MHD two-dimensional mass plus heat transfer motion of a viscous, radiating, heat conductive, chemical reacting and radiation Kuvshinsky's fluid past a porous media over a half-infinite vertical plate. The assumptions below are made in the formulation of this problem:

(1) An unsteadiness, laminar motion is elucidated;
(2) Induced magnetic field is avoided because magnetism Reynold's number andtransversely imposed magnetism was utilized to be small;
(3) Thermal-diffusion plus diffusion-thermo are surmized to be of substantial magnitude, hence, they can not be avoided;
(4) The penetrable plate is of infinite length in x^*-direction.
(5) In as much the motion of liquid is presumed to be within direction of x-direction,the physical quantities are functions of y^* and t^* only.

(iv) In the flow field, pressure is taken to be constant; and

(vii) Finitely conducting fluid with physical attributes which is constant was observed.
.
The Dimensional Governing Equation. With the above assumptions, the governing equations (Gurudatt Sharma et al., 2013 and Uwanta et al.,2015) of the flow in the vertical porous plate are:

Continuity equation.

$$\frac{\partial v^*}{\partial y^*} = 0 \tag{1.1}$$

Momentum equation.

$$\begin{cases} \left(1+\lambda^*\frac{\partial}{\partial t}\right)\frac{\partial u^*}{\partial t^*} + \nu^*\frac{\partial u^*}{\partial y^{*2}} = \nu^*\frac{\partial^2 u^*}{\partial y^{*2}} + g\beta^*\left(T^*-T_\infty\right) + g\beta^*\left(C-C_\infty\right) - \\ \left(1+\lambda^*\frac{\partial}{\partial t}\right)\left(\frac{\sigma}{\rho}B_0^2 + \frac{\nu}{K^*}\right)u^* - \frac{bu^{*2}}{\rho k} \end{cases} \tag{1.2}$$

Energy equation.

$$\begin{array}{l} \left(1+\lambda^*\frac{\partial}{\partial t}\right)\frac{\partial T^*}{\partial t^*} + \nu^*\frac{\partial T^*}{\partial y^{*2}} = \frac{k}{\rho C_\rho}\frac{\partial}{\partial y^*}\left\{\left[1+m\left(T^*-T_\infty\right)\right]\frac{\partial T^*}{\partial y^*}\right\} \\ -\frac{1}{\rho C_\rho}\frac{\partial q_r}{\partial y^*} + \frac{\alpha_T}{\rho C_\rho}\left(T^*-T_\infty\right) + \frac{D_m K_T \partial^2 C^*}{C_\rho \partial y^{*2}} \end{array} \tag{1.3}$$

Concentration equation.

$$\frac{\partial C^*}{\partial t^*} + \nu^*\frac{\partial C^*}{\partial y^*} = D_m\frac{\partial^2 C^*}{\partial y^{*2}} - R^*\left(C^*-C_\infty\right) + \frac{D_m K_T \partial^2 T^*}{T_m \partial y^{*2}} \tag{1.4}$$

The boundary conditions for the velocity, temperature and concentration fields are:

$$\begin{cases} t^* \le 0,\ u^* = 0, T^* \to T_{\infty^*}, C^* \to C_{\infty^*}\ for\ all\ y^*, \\ t^* > 0,\ u^* = 0, T^* \to T_{\infty^*}, C^* \to C_{\infty^*}\ at\ y^* = 0, \\ u^* = 0, T^* = T_0, C^* = C_0\ at\ y^* = 1. \end{cases} \tag{1.5}$$

1.1. **Non-Dimensional Variable.** We added the following quantities into equations to resolve the governing equations in dimensional-free form:

$$\begin{cases} u = \frac{u}{u_0}, y = \frac{V_0 y^*}{\nu}, t = \frac{V_0^2 t^*}{\nu}, \theta = \frac{T^*-T_\infty}{T_w-T_\infty}, C = \frac{\phi^*-\phi_\infty}{\phi_w-\phi_\infty}, P_r = \frac{\nu\rho C_\rho}{K} = \frac{\nu}{\alpha}, \\ Gr = \frac{g\beta\nu(T_w-T_\infty)}{V_0^3}, Gc = \frac{g\beta\nu(\phi_w-\phi_\infty)}{V_0^3}, M = \frac{\nu\sigma B_0^2 u}{\rho V_0^2}, \alpha_T = \frac{\nu^2 Q_T}{V_0^2 K_0}, \\ K_r = \frac{\nu R^*(\phi_w^*-\phi_\infty^*)}{V_0^2}, R = \frac{4I_1\nu(T^*-T_\infty^*)}{KV_0^3}, Fs = \frac{b^* u_0}{V_0^2\nu}, Du = \frac{D_m K_T(\phi_w^*-\phi_\infty^*)}{C_s C_\rho \nu(T_w^*-T_\infty^*)}, \\ \lambda = \frac{\lambda^* u_0 V_0^2}{\nu}, N = \left(M+\frac{1}{K}\right), \tau = m\left(T_w-T_\infty\right), Da = \frac{K^* u}{V_0^2\nu}. \end{cases} \tag{1.6}$$

Non-Dimensional Governing Equation. The above governing equations (1.2), (1.3), (1.4) and (1.5) in dimensionless form are:

$$\begin{cases} \left(1+\lambda\frac{\partial}{\partial t}\right)\frac{\partial u}{\partial t} - \left(1+\varepsilon A e^{nt}\right)\frac{\partial u}{\partial y} = \\ \frac{\partial^2 u}{\partial y^2} + G_r\theta + G_c C - \left(M+\frac{Fs}{Da}\right)\left(1+\lambda\frac{\partial}{\partial t}\right)u - \frac{1}{Da}u. \end{cases} \tag{1.7}$$

$$\begin{cases} \left(1+\lambda\frac{\partial}{\partial t}\right)\frac{\partial \theta}{\partial t} - \left(1+\varepsilon A e^{nt}\right)\frac{\partial \theta}{\partial y} = \\ \frac{1}{\mathrm{Pr}}\left(1+\tau\theta\right)\frac{\partial^2\theta}{\partial y^2} + \frac{\tau}{\mathrm{Pr}}\left(\frac{\partial\theta}{\partial y}\right)^2 - \left(R-Q\right)\theta + Du\frac{\partial^2 C}{\partial y^2} \end{cases} \tag{1.8}$$

$$\frac{\partial C}{\partial t} - \left(1 + \varepsilon A e^{nt}\right) \frac{\partial C}{\partial y} = \frac{1}{Sc} \frac{\partial^2 C}{\partial y^2} + S_r \frac{\partial^2}{\partial y^2} - K_r C \tag{1.9}$$

The boundary conditions (1.5) are given by the following dimensionless form:

$$\begin{cases} t^* \leq 0,\ u^* = 0,\ \theta^* = 0,\ c^* = 0,\ forall\ y^*, \\ t^* > 0,\ u = 0,\ \theta = 1,\ c = 1,\ aty = 0, \\ u = 0,\ \theta = 0,\ c = 0,\ at\ y = 1. \end{cases} \tag{1.10}$$

2. Method of Solution

The finite differential approach of Crank-Nicolson is utilized for numeric resolution, utilizing a finite differential implicit methodology, of coupling nonlinear partial differential equations (1.7)-(1.9), as well as the initial and boundary terms (1.10). The equivalent approximations to the equations (1.7)-(1.10) are the equivalent approximations of the limited difference (1.7)-(1.10):

Momentum equation.

$$\begin{cases} 1 + \frac{\lambda}{\Delta t} \frac{U_i^{j+1} - U_i^j}{\Delta t} - 1 + \varepsilon A e^{nt} \frac{U_{i+1}^{j+1} - U_{i-1}^{j+1`}}{2\Delta y} \\ = \frac{\left(U_{i+1}^{j+1} - 2U_i^{j+1} + U_{i+1}^j + U_{i+1}^j - 2U_i^j + U_{i-1}^j\right)}{(2\Delta y^2)} \\ + Gr\left(\theta_i^j\right) + Gc\left(C_i^j\right) - \left(1 + \frac{\lambda}{\Delta t}\right)\left(M + \frac{Fs}{Da}\right)\left(U_i^j\right)^2 - \frac{1}{Da}\left(U_i^j\right) \\ - A_1 U_{ij+1} + A_2 U_{ij+1} - A_1 U_{ij+1} = \\ A_3 U_{ij-1} + A_4 U_{ij} + A_6 U_{ij+1} - A_5 U_{ij} + A_7 \theta_{ij} + A_8 C_{ij}. \end{cases} \tag{2.1}$$

where

$$\begin{cases} A_1 = r_2, A_2 = 2(G + r_2), A_3 = (r_2 - r_1 B), A_4 = (2G - 2r_2 - r_4), \\ A_5 = r_5, A_6 = (r_1 B + r_2), A_7 = r_6, A_8 = r_7. \end{cases} \tag{2.2}$$

Energy equation.

$$\begin{cases} \left(1 + \frac{\lambda}{\Delta t}\right) \frac{\Pr}{\Delta t} \left(\theta_i^{j+1} - \theta_i^j\right) - \Pr\left(1 + \varepsilon A e^{nt}\right) \left(\frac{\theta_{i+1}^{j+1} - \theta_{i-1}^{j+1} + \theta_{i+1}^j - \theta_{i-1}^j}{2\Delta y}\right) = \\ \frac{q}{2\Delta y^2} \left(\theta_{i+1}^{j+1} - 2\theta_i^{j+1} + \theta_{i-1}^{j+1} + \theta_{i+1}^j - 2\theta_i^j + \theta_{i-1}^j\right)^2 \\ - (R - Q) \left(\frac{\theta_{i+1}^{j+1} + \theta_i^j}{2}\right) + \frac{Du \Pr}{2(\Delta y)^2} \left(C_{i+1}^{j+1} - 2C_i^{j+1} + C_{i-1}^{j+1} + C_{i+1}^j - 2C_i^j + C_{i-1}^j\right) \\ \left(1 + \frac{\lambda}{\Delta t}\right) \frac{\Pr}{\Delta t} \left(\theta_i^{j+1} - \theta_i^j\right) - \Pr\left(1 + \varepsilon A e^{nt}\right) \left(\frac{\theta_{i+1}^{j+1} - \theta_{i-1}^{j+1} + \theta_{i+1}^j - \theta_{i-1}^j}{2\Delta y}\right) = \\ \frac{q}{2\Delta y^2} \left(\theta_{i+1}^{j+1} - 2\theta_i^{j+1} + \theta_{i-1}^{j+1} + \theta_{i+1}^j - 2\theta_i^j + \theta_{i-1}^j\right)^2 \\ - (R - Q) \left(\frac{\theta_{i+1}^{j+1} + \theta_i^j}{2}\right) + \frac{Du \Pr}{2(\Delta y)^2} \left(C_{i+1}^{j+1} - 2C_i^{j+1} + C_{i-1}^{j+1} + C_{i+1}^j - 2C_i^j + C_{i-1}^j\right) \end{cases} \tag{2.3}$$

$$\begin{cases} -B_1\theta_{i-1}^{j+1} + B_2\theta_i^{j+1} - B_1\theta_{i+1}^{j+1} = B_3\theta_{i-1}^{j} + B_4\theta_i^{j} + B_5\theta_{i+1}^{j} + \\ B_6\left(\theta_{i+1}^{j} - \theta_{i-1}^{j}\right)^2 + B_7\left(C_{i+1}^{j+1} - 2C_i^{j+1} + C_{i-1}^{j+1} + C_{i+1}^{j} - 2C_i^{j} + C_{i-1}^{j}\right). \\ B_1 = r_2H, B_2 = 2\left(\Pr G + r_2H\right), B_3 = \left(Hr_2 - B\Pr r_1\right), \\ B_4 = \left(2\Pr G - 2r_2H\right), B_5 = \left(r_2H + r_1B\Pr\right), B_6 = 2rr_2a_2, B_7 = r_2r_{10}. \end{cases} \tag{2.4}$$

Concentration equation.

$$\begin{cases} \left(\frac{C_i^{j+1} - C_i^{j}}{\Delta t}\right) - \left(1 + \varepsilon Ae^{nt}\right)\left(\frac{C_{i+1}^{j+1} - C_{i-1}^{j+1} + C_{i+1}^{j} - C_{i-1}^{j}}{2\Delta y}\right) \\ = \frac{q}{2\Delta y^2}\left(\frac{C_{i+1}^{j+1} - 2C_i^{j+1} + C_{i-1}^{j+1} + C_{i+1}^{j} - 2C_i^{j} + C_{i-1}^{j}}{Sc}\right) \\ -K_r + S_r\left(\theta_{i+1}^{j+1} - 2\theta_i^{j+1} + \theta_{i-1}^{j+1} + \theta_{i+1}^{j} - 2\theta C_i^{j} + \theta_{i-1}^{j}\right) \end{cases} \tag{2.5}$$

$$\begin{cases} -D_1C_{i-1}^{j+1} + D_2C_i^{j+1} - D_1C_{i+1}^{j+1} = D_3C_{i-1}^{j} + D_4C_i^{j} + D_5C_{i+1}^{j} + D_6C_i^{j}. \\ D_1 = r_2, D_2 = 2\left(Sc + r_2\right), D_3 = \left(r_2 - r_1 - BSc\right), D_4 = 2\left(Sc - r_2\right), \\ D_5 = \left(r_2 + r_1 + BSc\right), D_6 = r_{11}, \end{cases} \tag{2.6}$$

Note that:

$$\begin{cases} H\left(1 + \tau\theta_i^{j}\right), B\left(1 + \varepsilon Ae^{nt}\right), G = \left(1 + \lambda\frac{\partial}{\partial t}\right), r_1 = \frac{\Delta t}{\Delta y}, r_2 = \frac{\Delta t}{(\Delta y)^2}, \\ r_3 = 2\Delta t, r_4 = r_3GM, r_5 = r_3\frac{G}{K}, r_6 = r_3G_r, r_7 = r_3G_c, r_8 = 2\lambda r_2, \\ r_9 = r_3\left(R - Q\right), r_{10} = Dur_2\Pr, r_{11} = r_3ScK_r \end{cases} \tag{2.7}$$

$$\begin{cases} U_{i,j} = 0, \theta_{i,j} = 0, C_{i,j} = 0 \ for \ all \ y = 0 \\ U_{0,j} = 0, \theta_{0,j} = 1, C_{0,j} = 1 \\ U_{L,j} \to 0, \theta_{L,j} \to 0, C_{L,j} \to 0 \end{cases} \tag{2.8}$$

The i and j indices relate to space and time co-ordinates. The mesh sizes for the y direction and t time are indicated by the Δy and Δt variables correspondingly. Numerical computations for a range of potential values are carried out for each of the physical parameters involved in the question. The finite differences equations (2.3) (2.5) create a tridiagonal system of equations at each internal nodal point at a certain n-level, which may be resolved by applying the Thomas Algorithm.
In each step the concentration and temperature profiles were calculated first using equations (2.3) and (2.5), then the calculation results were used to construct the speed profile which satisfies in each instance the convergence criteria. Skin-friction C_f is
provided by Nusselt Number Nu and Sherwood Number Sh and

$$C_f = \left(\frac{\partial u}{\partial y}\right)_{y=0}, Nu = -\left(\frac{\partial \theta}{\partial y}\right)_{y=0}, Sh = \left(\frac{\partial c}{\partial y}\right)_{y=0}$$

3. Results and Discussion of the Findings

In order to obtain a physical view of the current work, an efficient numerical method known as the Crank-Nicolson method, in conjunction with MATLAB programming, has been used to solve the transformed equations (11, 13 and 15) subject to the boundary conditions of equations (3.68-3.70) in order to obtain a physical view of the present work (2.8). Graphs and tables displaying numerical results for velocity profiles (u), temperature

profiles (T), concentration profiles (C), skin friction (C_f), rate of heat transfer in terms of Nusselt number (Nu), and rate of mass transfer in terms of Sherwood number (Sh) have been created by assigning numerical values to different values of pertinent parameters. To conduct the study, the following values are used: $Gr = 1.0, Gc = 1.0, M = 1, K = 0.1, Pr = 0.71, Sc = 0.60, R = 1, Kr = 0.5, tau = 0.01, lambda = 0.0002, Sr = 0.5, Da = 0.1$.

4.2.1 Velocity Profiles. The impact on velocity of different Grashof thermal values are shown in Figures 4.2 and 4.3. It is worth noting that the speed rises with increasing value of the thermal Grashof. The link between the Grashof mass number and the speed will be discussed below. It has been observed that the speed increases with the bulk of Grashof. It has been shown that greater surface cooling (i.e. Gr and Gc) leads to an increase in air flow speed. This is because an increase in the Grashof thermal numbers and the Grashof mass numbers may improve thermal and mass boost effects. As a consequence, the induced flow will rise. The dimensionless speed increases as the Darcy number increases in the equation. It may be seen. Larger Da parameter values are correlated with larger porous medium permeability that is less porous, implying lower fiber flow resistance and therefore increased transport acceleration (figure 4.4).

Figure 4.5 shows that the increase in the Fs parameter increases the flow resistance and therefore reduces the profile of the speed. The link between speed and viskoelastic parameter is shown by figure 4.5. The normal flow stress coefficient is the viscoelastic flow parameter. Figure 4.6 shows that the velocity rises as the viscoelastic parameter increases at a particular point on the flow domain. This is theory compatible. As demonstrated in Fig. 4.7, the increase in the parameter (M) causes the fluid speed to decline. The effect of a magnetic transverse field on electric fluid substantially slows the velocity of the fluid. This is because a transverse magnetic field is applied, which produces a resistive force (Lorentz force). The force is comparable to the drag force since it is intended to counteract fluid flux and at the same time decrease fluid speed.

Figure 4.8 shows the speed profiles for the various Prandtl numbers. This image shows that the speed decreases as the number of Prandtl grows in the system. This is thus physical because the Prandtl number reflects the connection between momentum diffusivity (kinetic viscosity) and heat diffusivity. This number indicates a dimensionless number. In a wide range of heat transport problems, the Prandtl number controls the relative thickness of momentum and thermo-boundary layers. If Pr is small, then the heat is very quickly diffused compared with speed (momentum). This means the thickness of the temperature limit layer is much higher than that of the velocity limit layer for liquid metals.

The speed profile for different R values is described in this Figure 9. The speed profile is reduced when R in this example is raised. A higher R value shows a better control over radiation, resulting in reduced both the buoyancy strength and density of the limit layer of the momentum. A higher R value shows an increased driving dominance over radiation. Figure 10 indicates that Sc's value increases proportionately as the velocity profile decreases. Furthermore, the velocity decreases as shown by an increase in the suction parameter α (Figure 11). This is because the suction parameter causes fluid particles to decelerate as the pore wall passes and therefore reduces fluid boundary layer growth.

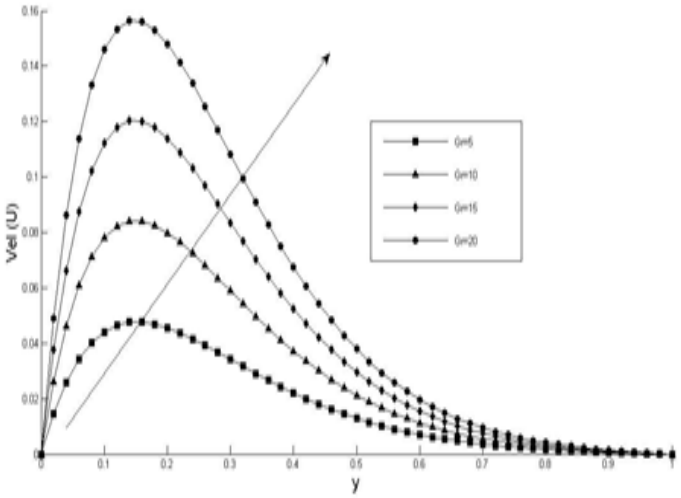

Figure 1: Contribution of Grashof number on Velocity

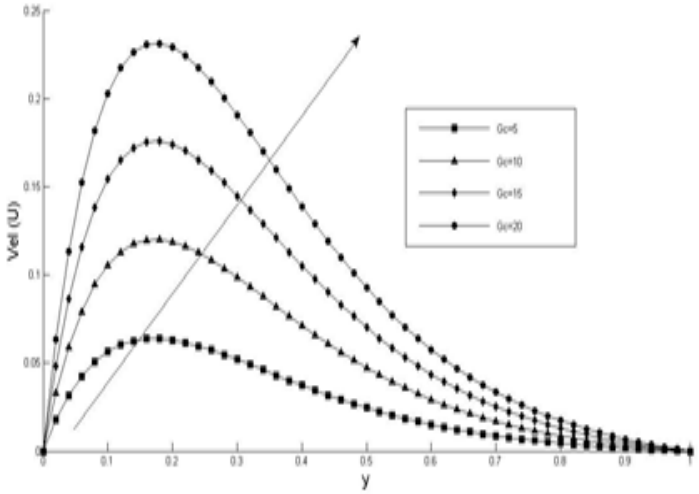

Figure 2: Contribution of mass Grashof number on Velocity

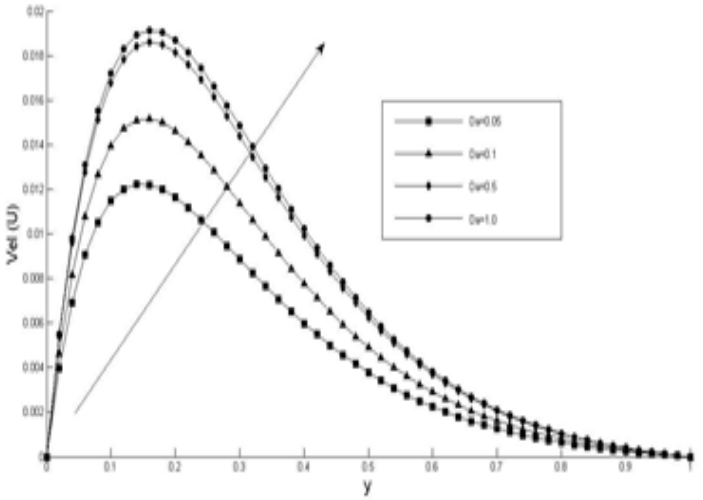

Figure 3: Contribution of Da on Velocity

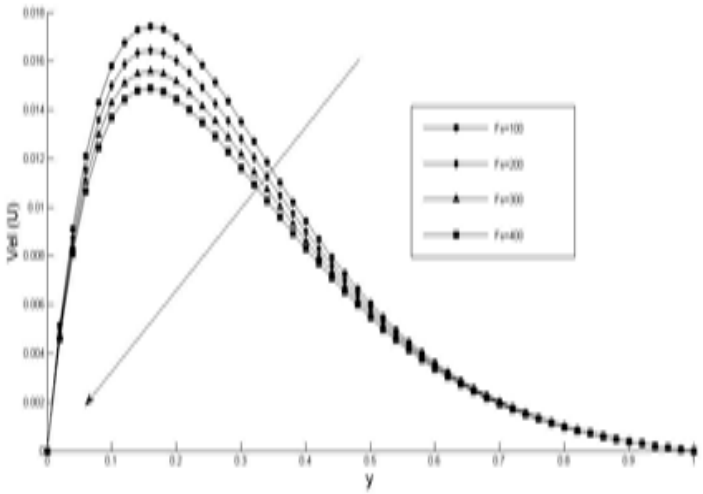

Figure 4: Contribution of Fs on Velocity

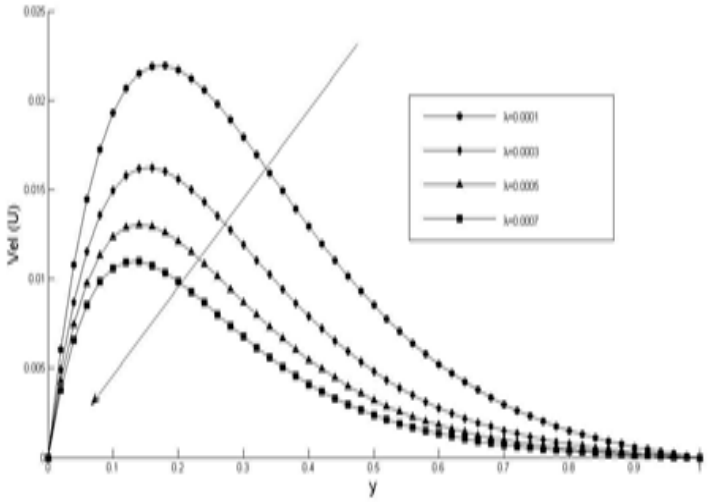

Figure 5: Contribution of λ on Velocity

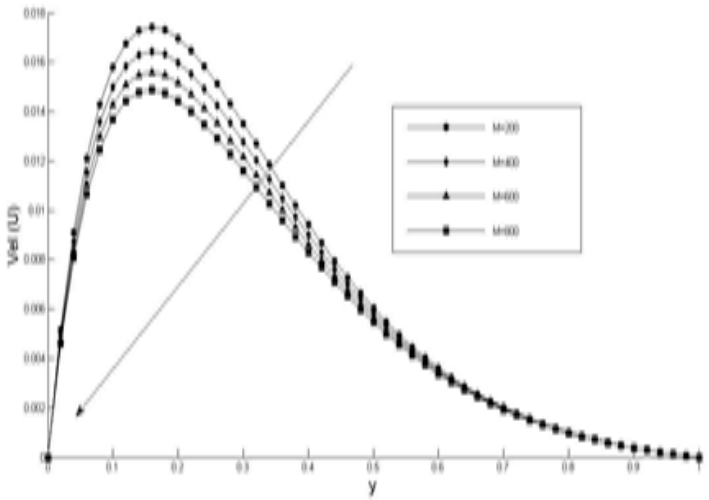

Figure 6: Contribution of Magnetic parameter on Velocity

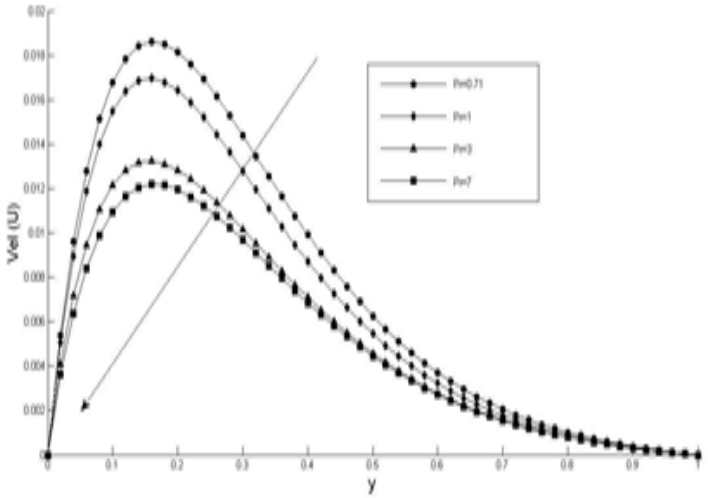

Figure 7: Contribution of Prandtl on Velocity

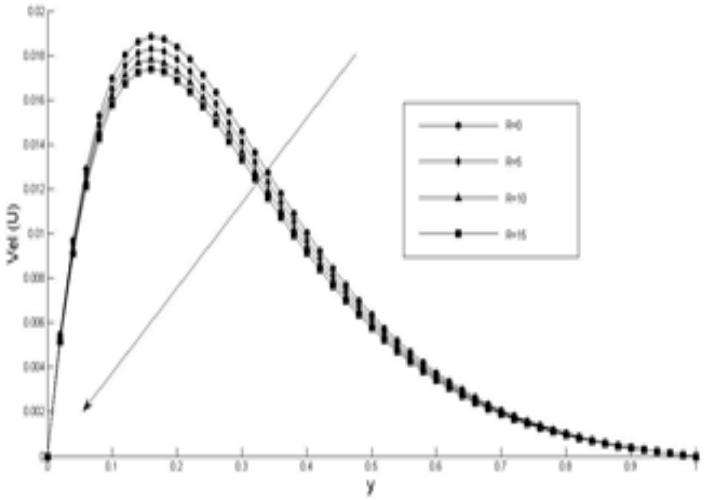

Figure 8: Contribution of Radiation on Velocity

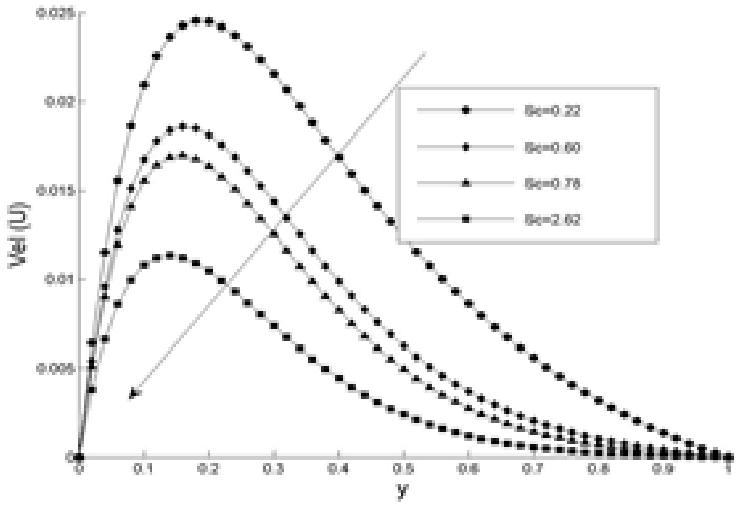

Figure 9: Contribution of Schmidt on Velocity

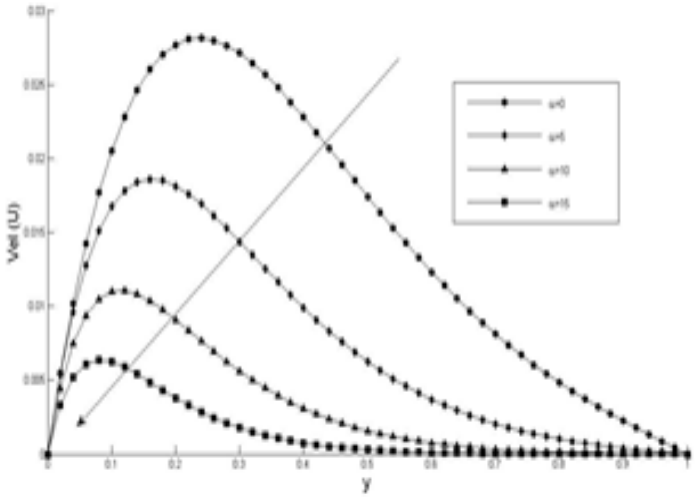

Figure 10: Contribution of α on Velocity

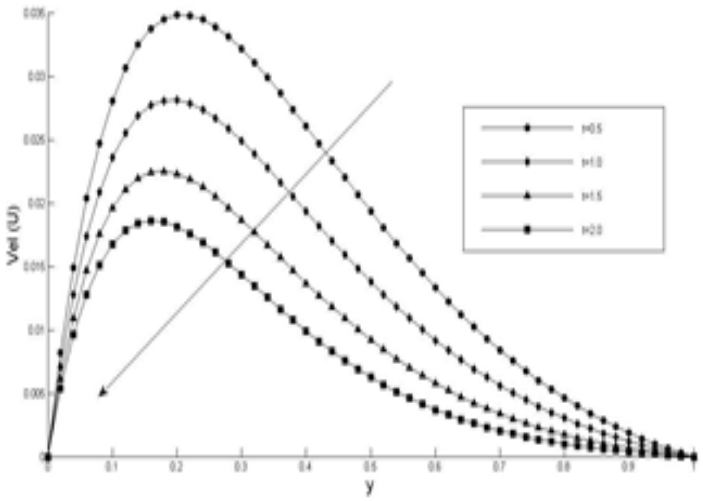

Figure 11: Contribution of t on Velocity

3.1. **Temperature Profiles.** In Figure 13, the impact of the Dufour number (Du) on temperature profiles is shown. It has been noticed that the temperature rises in direct proportion to the Dufour number.
As shown in Figure 13, the impact of the λ on the temperature profile may be observed. It is noticed that the temperature profile drops as the value of λ rises in magnitude. The effects of Pr on the temperature profile are shown in Figure 4.14. It has been observed that the temperature lowers as the concentration of Pr increases. Figure 4.15 shows that temperature rises as Q increases, as can be seen in the graph. Figure 4.16 depicts the fluctuation of the temperature component over a range of values of the constant R. The outcome demonstrates that the impact of increasing R values leads in a decrease in the temperature distribution profile. The impact of a changing suction parameter on the temperature profile is shown in Figure 4.17. During our research, we found that the suction parameter α rises in direct proportion to the temperature profile. Figure 4.18 illustrates how the impact of the thermal conductivity parameter τ grows as the temperature profile progresses.

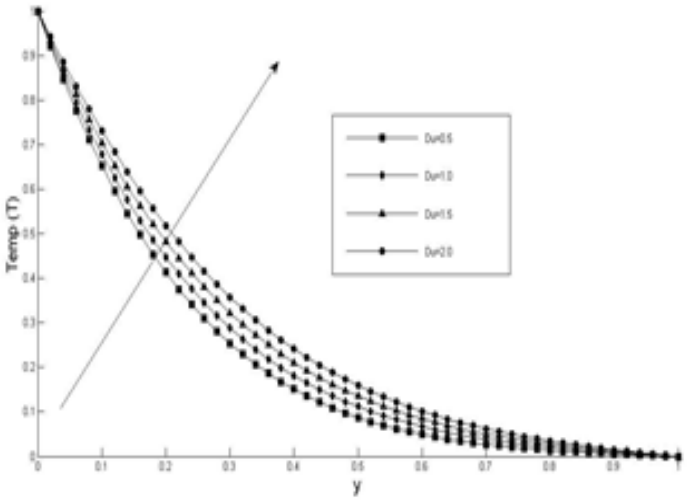

Figure 12: Contribution of Dufour number on Temperature

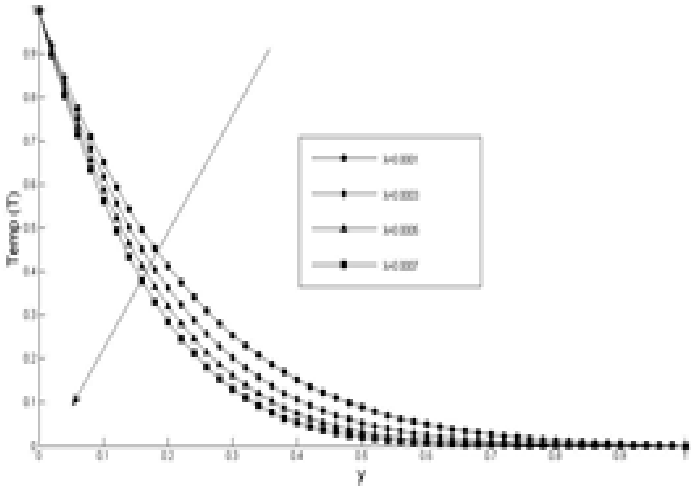

Figure 13: Contribution of λ on Temperature

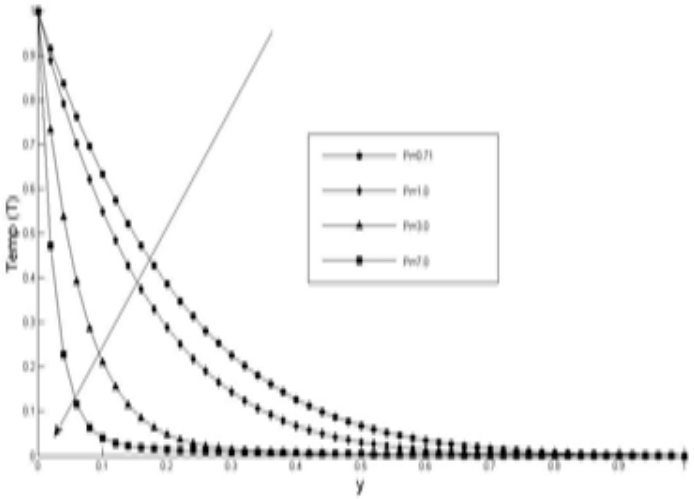

Figure 14: Contribution of Prandtl number on Temperature

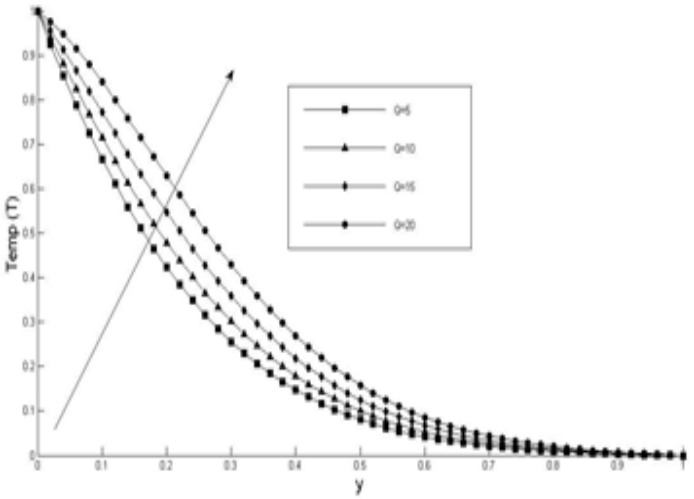

Figure 15: Contribution of heat generation on Temperature

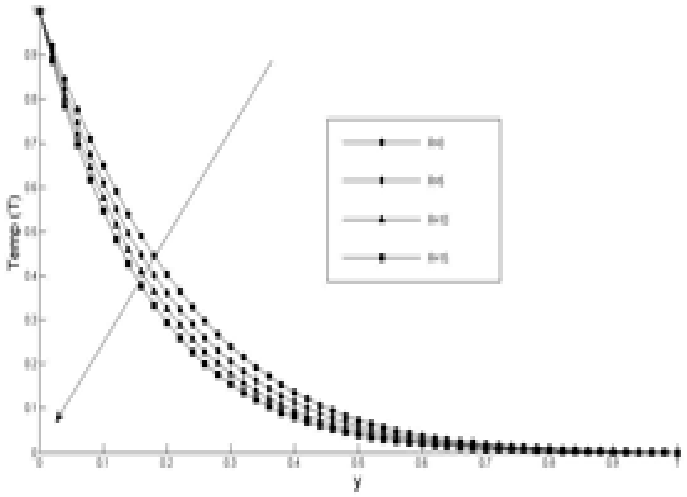

Figure 16: Contribution of Radiation on Temperature

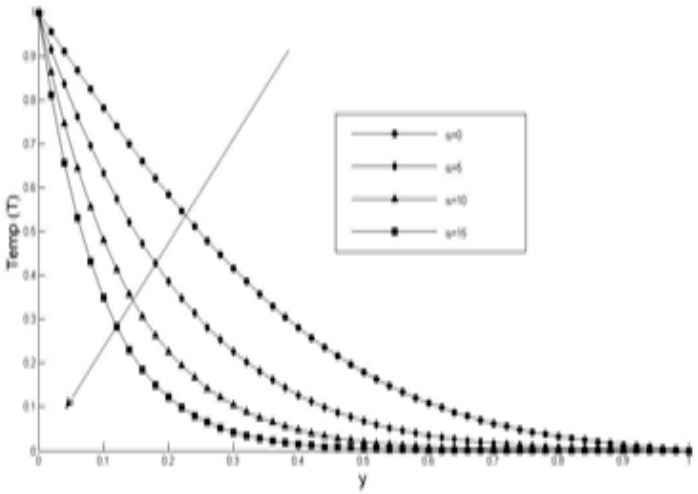

Figure 17: Contribution of α on Temperature

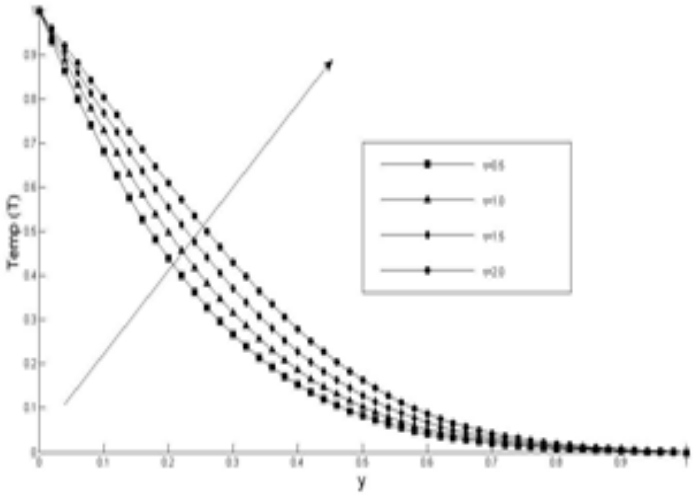

Figure 18: Contribution of τ on Temperature

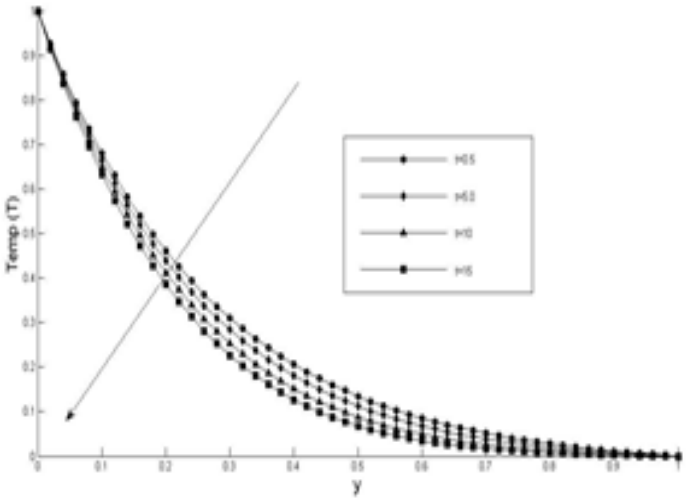

Figure 19: Contribution of t on Temperature

3.2. **Concentration Profiles.** In Figures 20, 21, and 22, the concentration profiles for various values of the Schmidt number (Sc), the Schmidt ratio (Sr), and the Chemical reaction (Kr) are shown. The effect of Schmidt number Sc and chemical reaction on concentration is shown in Figures 20 and 21, respectively. As the Schmidt number rises, the concentration profile becomes more and more pronounced. It should also be observed that when the Schmidt number rises, the concentration boundary layer gets more thin. When the concentration buoyancy effect decreases, the fluid concentration decreases as a result of the decreased concentration. In terms of physics, a rise in Sc corresponds to a reduction in molecular diffusivity. The concentration, on the other hand, falls as the chemical reaction Kr increases. In a similar vein, when the chemical reaction parameter rises, the concentration boundary barrier gets thinner and thinner. Figure 22 shows the effect of the (Sr) parameter, which shows that when the Soret parameter increases, the concentration profile increases as well.

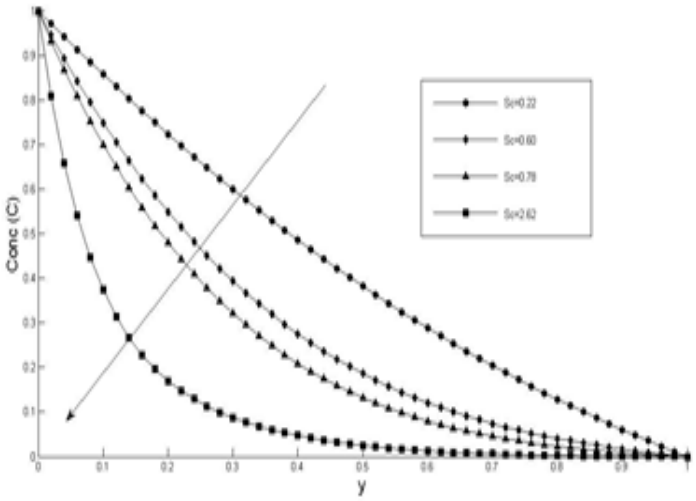

Figure 20: Contribution of Schmidt number on Concentration

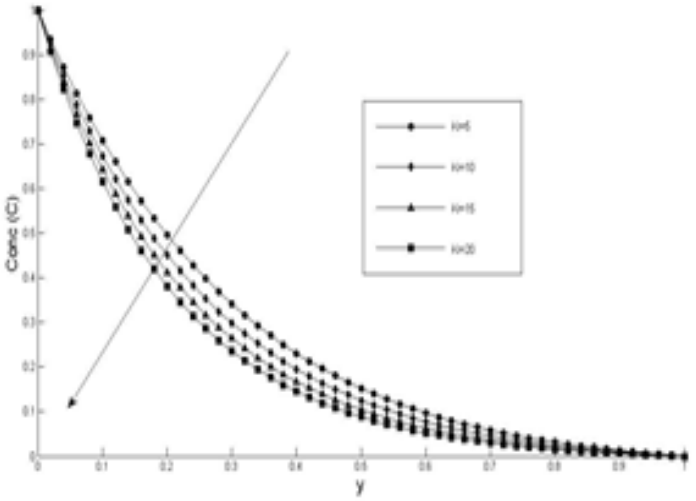

Figure 21: Contribution of chemical reaction on Concentration

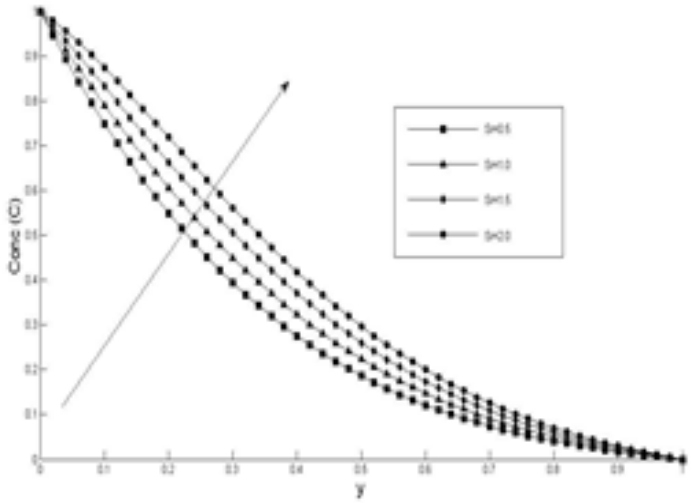

Figure 22: Contribution of Soret number on Velocity

3.3. **Table of Values.** Tables 4.1 and 4.2 demonstrate a comparison between the current study and the work of Uwanta and Halima (2015) in terms of findings. In the absence of Viscoelastic(Kuvshinshiki type) and heat source parameters, the effects of the thermal conductivity parameter on Skin frcition and Nusselt number were observed. The results obtained in this work are a more generalized form of the results obtained by Uwanta et al.[2015] and can be taken as a limiting case by taking λ and Q =0. Interestingly, the current findings, as shown in Tables 4.1 and 4.2, are in good agreement with the results obtained by Uwanta et al.[2015] when the viscoelastic and heat source parameters are not taken into consideration. That the current answer is correct and that the numerical technique was used to arrive at it is shown by these results. Furthermore, we show the computational results for the skinfriction coefficient, the Nusselt number, and the Sherwood number for various values of (M, λ, Fs, R, Pr, τ, α,Kr,Sc,Gr, Gc, Da) and the skin-friction coefficient, Nusselt number, and Sherwood number. It was discovered that increasing the λ parameter increased the Skin friction coefficient, while decreasing the Nusselt number was seen for Pr=0.71 and 7.0, respectively. Various thermophysical characteristics such as skin friction, Nusselt number, and Sherwood number are presented in Tables 4.3-4.7 as well as their impacts on skin friction and Nusselt number. It has been seen from Tables 4.3-4.4 that skin friction rises with an increase in Gr, Gc, Da, and α, which explains why the (M, λ, Fs, R, and Pr) decreased in value. However, it should be noted that when the (λ, R, Pr, τ, α) are raised, there is no statistically significant change in the Nusselt number. Q and Du, on the other hand, rise when the Nusselt number increases in Tables 4.5-4.6. Numbers representing the numerical values for Sc, Kr, and Sr are shown in Table 4.7. Because of the rising values of Sc and Kr, the Sherwood number falls. When the Sr parameter is raised, there is a statistically significant change in the Sherwood number.

Table-4.1: Numerical values for skin-friction coefficient C_f and Nusselt number N_u for various values of thermal conductivity compared with Uwanta and Halima (2015); $Gr = Gc = 1.0, Pr = 0.71, Sc = 0.60, \alpha = 0.5, n = 0.1, M = 1.0, \epsilon = 0.02, R = 0.1, Da = 0.5, Fs = 1.0, Du = 0.1, \lambda = 0, Sr = 0, Q = 0.$

	Present Work		Uwanta and Halima(2015)	
T	C_f	N_u	C_f	N_u
0.0	0.2774	1.5634	0.2820	1.5656
0.005	0.2779	1.5264	0.2826	1.5276
0.1	0.2785	1.4905	0.2832	1.4908
0.20	0.2796	1.4218	0.2843	1.4207
0.25	0.2801	1.3890	0.2848	1.3872
0.3	0.2807	1.3571	0.2854	1.3547

Table 4.2: Numerical values for skin-friction coefficient C_f and Nusselt number N_u for various values of thermal conductivity compared with Uwanta and Halima(2015); $Gr = Gc = 1.0, Pr = 0.70, Sc = 0.60, \alpha = 0.5, n = 0.1, M = 1.0, \epsilon = 0.02, R = 0.1, Da = 0.5, Fs = 1.0, Du = 0.1, \lambda = 0, Sr = 0, Q = 0$.

	Present Work		Uwanta and Halima(2015)	
T	C_f	N_u	C_f	N_u
0.0	0.2310	5.1090	0.2360	5.1088
0.005	0.2314	4.9959	0.2363	4.9952
0.1	0.2317	4.8851	0.2367	4.8839
0.20	0.2324	4.46705	0.2374	4.4682
0.25	0.2328	4.5667	0.2377	4.5638
0.3	0.2331	4.4652	0.2381	4.4617

Table 4.3: Influence of Gr, Gc and M on the Skin friction, Nusselt number and Shewrwood number for various parameters when $Sc = 0.60, \tau = 0.01, \lambda = 0.0002, Pr = 0.71, Q = 1, Du = 0.1, Da = 0.5, Fs = 1, R = 2, Sr = 0.5, n = 1, \epsilon = 0.02$.

Gr	Gc	M	C_f	N_u	S_h
5	1	1	0.8168	−4.4018	−2.7955
10	1	1	1.4617	−4.4018	−2.7955
15	1	1	2.1052	−4.4018	−2.7955
1	5	1	0.9782	−4.4018	−2.7955
1	10	1	1.8228	−4.4018	−2.7955
1	15	1	2.6635	−4.4018	−2.7955
1	1	200	0.2866	−4.4018	−2.7955
1	1	400	0.2756	−4.4018	−2.7955
1	1	600	0.2661	−4.4018	−2.7955

Table-4.4: Effect of Da, λ and Fs on the Skin friction, Nusselt number and Shewrwood number for various parameters when $M = Gr = Gc = 1, Sc = 0.60, \tau = 0.01, \lambda = 0.0002, Pr = 0.71, Q = 1, Du = 0.1, Da = 0.5, R = 2, Sr = 0.5, n = 1, \epsilon = 0.02$.

Da	Λ	Fs	C_f	N_u	S_h
0.05	0.0002	1	0.2239	−4.4018	−2.7955
0.1	0.0002	1	0.2594	−4.4018	−2.7955
0.5	0.0002	1	0.2996	−4.4018	−2.7955
0.5	0.0001	1	0.3329	−4.1929	−2.8293
0.5	0.0003	1	0.2749	−4.5999	−2.7642
0.5	0.0005	1	0.2399	−4.9655	−2.7073
0.5	0.0002	100	0.2866	−4.4018	−2.7955
0.5	0.0002	200	0.2756	−4.4018	−2.7955
0.5	0.0002	300	0.2662	−4.4018	−2.7955

Table-4.5:Numerical values of the Skin friction, Nusselt number and Shewrwood number for R, Q and Pr parameters when $M = Gr = Gc = 1, Sc = 0.60, \tau = 0.01, \lambda = 0.0002, Du = 0.1, Da = 0.5, Fs = 0.5, Sr = 0.5, n = 1, \epsilon = 0.02$.

R	Q	Pr	C_f	N_u	S_h
0	1	0.71	0.3022	−4.1213	−2.8360
5	1	0.71	0.2960	−4.7998	−2.7378
10	1	0.71	0.2906	−5.4102	−2.6488
1	5	0.71	0.3049	−3.8275	−2.8782
1	10	0.71	0.3123	−3.0267	−2.9923
1	15	0.71	0.3209	−2.1131	−3.1208
1	1	0.71	0.2996	−4.4018	−2.7955
1	1	1	0.2817	−5.7652	−2.5914
1	1	7	−0.2035	−33.5102	−1.1894

Table-4.6: Numerical values of the Skin friction, Nusselt number and Shewrwood number for various parameters (Du, τ, α) when $M = Gr = Gc = 1, Sc = 0.60, \lambda = 0.0002, Da = 0.5, Fs = 0.5, Sr = 0.5, Kr = 0.1, n = 1, \epsilon = 0.02$.

Du	τ	α	C_f	N_u	S_h
0.5	0.01	1	0.3050	−4.1275	−2.8365
1	0.001	1	0.3117	−3.7679	−2.8902
1.5	0.001	1	0.3186	−3.3883	−2.9469
0.1	0.5	1	0.3092	−3.5497	−2.9234
0.1	1	1	0.3194	−2.8764	−3.0246
0.1	1.5	1	0.3298	−2.3638	−3.1019
0.1	0.01	0	0.2923	−2.2519	−1.1962
0.1	0.01	5	0.2996	−4.4018	−2.7955
0.1	0.01	10	0.2583	−7.2204	−4.9955

Table 4.7: Numerical values of the Skin friction, Nusselt number and Shewrwood number for various parameters (Sc, Kr, Sr) when $M = Gr = Gc = 1, Sc = 0.60, \tau = 0.01, \lambda = 0.0002, Du = 0.1, Da = 0.5, Fs = 0.5, n = 1, \epsilon = 0.02$.

Sc	Kr	Sr	C_f	N_u	S_h
0.22	0.1	0.5	0.3533	−4.4469	−1.4647
0.60	0.1	0.5	0.2996	−4.4018	−2.7955
0.78	0.1	0.5	0.2836	−4.3791	−3.4830
0.60	5	0.5	0.2905	−4.3830	−3.4039
0.60	10	0.5	0.2825	−4.3658	−4.9447
0.60	15	0.5	0.2755	−4.3503	−4.4233
0.60	0.1	1.0	0.3120	−4.4219	−2.2007
0.60	0.1	1.5	0.3244	−4.4422	−1.5999
0.60	0.1	2.0	0.3368	−4.4627	−0.9928

Conclusions: The viscous and thermal conductivity fluid parameters involved in this study have significant effects on the fluid flows. The key findings are as follows:

(1) The velocity profile upsurge with an increase in E_c, τ,Du and b while it decreases with an increases in λ and K_r. It is obvious from our outcomes that viscous dissipation speed up the convective motion.

(1) Both the velocity and temperature profiles declines with a higher values of E_c, τ, Du, S_r and R and K_r.
(2) The concentration figures inclined with a considerable values of K_r and λ.

(3) It is detected that skin-friction coefficient enhanced with a considerable values of Gr, Gc, Da and Fs while is weakened the λ, M and Ec.
(4) The Nulsselt values increase with an elevation in τ and Q but it is the other hand just revered subject to the Pr, R and λ.
(5) Increasing in Sc and Kr leads to fall of Sherwood number. There is a significant change in Sherwood number when the Sr parameter increased.

Acknowledgement: We acknowledged all authors we made reference to their works and thank all the authors of this work for their painstakingly contributed to the work. And thank our mentor Prof Gbadeyan for the opportunity to train under him.

Competing interests: The content of the manuscript was approved by all authors. Therefore, no competing interest between authors.

Funding: The Authors received no financial support for the research, authorship, and/or publication of this article.

References

[1] Idowu A. S., Dada M. S. & Jimoh A. (2013). Heat and mass transfer of Magnetohydrodynamic (MHD) and dissipative fluid flow pass a moving vertical porous plate with variable suction. *Mathematical Theory and Modeling*. **3**, 2224-5804.
[2] Moller M. M., Rahman A. & Rahman L. T. (2005). Natural convection flow from an isothermal sphere with temperature dependent thermal conductivity. *Journal of Naval Architecture and Marine Engineering*. **2** (2), 53-64.
[3] Raju G. & Siva P. R. (2016). Heat and Mass Transfer on MHD Free Convection Flow of Visco-Elastic Kuvshinshiki Fluid through Porous Medium past an Infinite Vertical Porous Plate. *IOSR Journal of Mathematics (IOSR-JM)*. 2278-5728.
[4] Uwanta I. J. & Halima U. (2014). Convective heat and mass transfer flow over a vertical plate with Nth order chemical reaction in a porous medium. *International Journal of Scientific Engineering and technology*. **3** (2), 172-185.
[5] Uwanta I. J. & Halima U. (2015). Finite difference solutions of magneto hydrodynamic free convective flow with constant suction and variable thermal conductivity in a Darcy-Forchheimer porous medium. *IOSR Journal of Mathematics*. **11**, 2278-5728.
[6] Oyelami F. H., Jimoh A. & Saka-Balogun O. Y. (2016).Finite difference method applied to an unsteady magnetohydrodynamic Newtonian fluid with wall slip in Darcy-Forchiemer porous medium. *International Journal of Mathematical Research*. **2**, 111-118.
[7] Agrawal V. P., Agrawal J. K. & Varshney N. K. (2012). Effect of stratified Kuvshinski fluid on MHD free convective flow past a vertical porous plate with heat and mass transfer. *Ultra Scientist*. **24** (1), 139-146.
[8] Arvind K. S., Dubey G. K. & Varshney N. K. (2012). Effect of Kuvshinski fluid on double-diffusive convection-radiation interaction on unsteady MHD flow over a vertical moving porous plate with heat generation and soret effects. *Advances in Applied Science Research*. **3**, 1784-1794.